Atmos. Meas. Tech. Discuss., 3, 2743–2778, 2010
www.atmos-meas-tech-discuss.net/3/2743/2010/
doi:10.5194/amtd-3-2743-2010


Atmospheric Measurement Techniques Discussions



# Aerosol Optical Depth measurements at 340 nm with a Brewer spectrophotometer and comparison with Cimel observations at Uccle, Belgium

**V. De Bock, H. De Backer, A. Mangold, and A. Delcloo**

Royal Meteorological Institute of Belgium, Ringlaan 3, 1180 Brussels, Belgium

Received: 28 May 2010 – Accepted: 21 June 2010 – Published: 29 June 2010

Correspondence to: V. De Bock (veerle.debock@meteo.be)

Published by Copernicus Publications on behalf of the European Geosciences Union.

## Abstract

The Langley Plot Method (LPM) is adapted for the retrieval of Aerosol Optical Depth (AOD) values at 340 nm from Brewer#178 sun scan measurements between 335 and 345 nm (convoluted with the band pass function of the Cimel filter at 340 nm). The use of sun scans instead of direct sun measurements simplifies the comparison of the AOD values with quasi-simultaneous Cimel values. Also, the intensities are larger at 340 nm due to lower ozone absorption, thus improving the signal to noise ratio. For the selection of the cloudless days, a new set of criteria is proposed. With the new method, individual clear sky AOD values, for which the selection criteria are also presented in this article, are calculated for a period from September 2006 to December 2009. These values are then compared to quasi-simultaneous Cimel measurements, showing a very good linear agreement (the correlation coefficient, the slope and the intercept are, respectively 0.960, 0.992 and 0.005), which proves that good quality observations can be obtained from Brewer sun scan measurements at 340 nm. The seasonal and monthly variability of the Brewer AODs at Uccle are consistent with other studies. The highest values can be observed in summer and spring. More than 50% of the winter AODs are lower than 0.3 whereas in summer, more than 50% of the values are larger than 0.5. On a monthly scale, the lowest AOD are observed in December and the highest values occur in June and April. No clear weekly cycle is observed for Uccle.

## 1 Introduction

Aerosols are particles in the solid or the liquid phase that are suspended in the atmosphere and have an important influence on the atmospheric chemistry and physics (Cheymol and De Backer, 2003; Raghavendra Kumar et al., 2010). They affect the tropospheric chemical composition, they can reduce visibility and they have important impacts on human health (Unger et al., 2009; Lyamani et al., 2010; Raghavendra Kumar et al., 2010). Aerosols also influence the Earth's radiation budget in a direct and indirect manner. The scattering and absorption of short and long wave radiation is called the direct effect (Kaufman et al., 2002; Ramanathan et al., 2001; Myrhe, 2009; Andreae et al., 2005). The indirect effect concerns the ability of aerosols to act as cloud condensation nuclei which influences the microphysical and optical properties of clouds, thus changing the radiative and precipitation properties and the lifetime of clouds (Kaufman et al., 2002; Ramanathan et al., 2001; Unger et al., 2009; Lohmann and Feichter, 2005; Lohmann, 2002). Because of a lack of information concerning the temporal and spatial distribution of aerosols, they are key contributors to the uncertainties in current climate studies (IPCC, 2007; Andreae et al., 2005).

Much attention has been paid to the influence of aerosols on ultraviolet (UV) radiation, since the impact of UV radiation on human health, the biosphere and atmospheric chemistry strongly depends on the characteristics and quantity of aerosol in the atmosphere. An overexposure to UV-B radiation can lead to serious health damage for humans such as skin cancer, accelerated aging of skin, cataract, photokeratitis (snow blindness) and changes in the immune system (Cordero et al., 2009; Rieder et al., 2008). UV-B radiation also has adverse effects on terrestrial plants. It can cause reduced growth, reduced photosynthetic activity and flowering (Cordero et al., 2009; Tevini and Teramura, 1989). Other elements of the biosphere are also influenced by UV-B radiation (e.g. inactivation of micro-organisms, reduction in food stocks for zooplankton; Diffey, 1991). There is increasing evidence that elevated UV-B radiation has significant effects on the terrestrial biosphere with implications for the cycling of carbon, nitrogen and other elements (UNEP, 2006). Increased UV-B is expected to enhance the concentration of hydroxyl radicals (OH) and results in faster removal of pollutants such as carbon monoxide (CO), methane ($CH_4$), non-methane hydrocarbons (NMHCs), sulphur and nitrogen oxides, hydrochlorofluorocarbons (HCFCs), and hydrofluorocarbons (HFCs) (Tang et al., 1998). The increase of anthropogenic aerosols in non-urban areas of the industrialized countries since the industrial revolution is supposed to have decreased the biologically active UV radiation by 5 to 18% (Liu et al.,





AMTD
3, 2743–2778, 2010

1991). Accuracy in UV prediction can be improved if the role of aerosols on surface UV radiation is clarified (Kim et al., 2008). However, little information is available on the optical properties of atmospheric aerosols in the UV spectral region, compared to the visible spectral range (Sellito et al., 2006).

To gain a better understanding of the effect of aerosols in the UV, knowledge of the parameters that determine the optical and physical properties of aerosols is essential (Cazorla et al., 2009). One of these parameters is the Aerosol Optical Depth (AOD), an integral measurement of the combined aerosol scattering and absorption in the atmospheric column (Mulcahy et al., 2009). Several reports have been written on the retrieval of AOD in the UV range. For example, Taylor et al. (2008) and Corr et al. (2009) use MFRSR (Multi Filter Rotating Shadowband Radiometer) measurements for this retrieval. Research also shows that the standard Brewer direct sun (DS) measurements allow AOD retrieval at the wavelengths used for ozone determination (mainly 320.1 nm). Some authors base their retrieval on the absolute calibration of the solar spectral irradiance measured by the Brewer (Marenco et al., 1997; Bais, 1997; Kazadzis et al., 2005) whereas others use the Langley extrapolation method to determine the absolute calibration of the irradiance (Marenco et al., 2002; Kirchhoff et al., 2001; Cheymol and De Backer, 2003). Arola and Koskela (2004) discussed the systematic errors in the AOD retrieval from Brewer DS measurements, which led to improvements of the conventional Langley Plot method (e.g., Cheymol et al., 2009). Several authors studied the spatial and temporal patterns in AOD. Both Xia et al. (2008) and Bäumer et al. (2008) reported a weekly cycle in AOD for Central Europe (45–55° N; 0–20° E). Seasonal patterns in AOD with maximum values in spring and summer and minimum values in autumn and winter are observed in many studies (Remer et al., 2008; Meleti and Cappellani, 2000; Behnert et al., 2004; Kim et al., 2006; Estellés, 2008; Léon et al., 2009; Che et al., 2009; Lyamani et al., 2010). Gröbner and Meleti (2004) studied long-term trends in AOD at Ispra and detected a decrease between 1991 and 1997, followed by a stabilization in the AOD values. Kazadzis et al. (2007) however, reported on a statistically significant (99% level) decrease in AOD for Thessa-





AMTD
3, 2743–2778, 2010

Ioniki after 1997. Hatzianastassiou et al. (2009) studied the spatial distribution of AOD over the Mediterranean basin.

In this paper, we present a new and improved method for the retrieval of AOD values. Instead of using the standard direct sun ozone measurements from the Brewer instrument (as in Cheymol and De Backer, 2003), we will use sun scan measurements between 335 and 345 nm, convoluted with the band pass function of the Cimel filter at 340 nm, to obtain AOD values at 340 nm. This will allow for a direct comparison between these retrieved AOD values and the AODs from the Cimel sun photometer at the same wavelength. Information about the used instruments and the measurement location is included in Sect. 2. The method applied for the retrieval of the Brewer AOD values is described in Sect. 3. The resulting AOD values are compared with Cimel measurements in Sect. 4. Also, the temporal patterns in AOD are discussed and compared to results of other studies.

## 2 Instruments and location

In this study, we make use of the measurements of a Brewer spectrophotometer and a Cimel sun photometer. Both instruments are located in Uccle, a residential suburb of Brussels about 100 km from the shore of the North Sea. The prevailing meteorological conditions will determine whether the station is influenced by sea salt aerosols, by aerosols from urban activity or by continental type of aerosols (De Backer, 2009).

The Brewer spectrophotometer was developed in the early 1980s to measure total ozone in the atmosphere from UV-B radiation (Brewer, 1973; Kerr et al., 1988). The instrument records raw photon counts of the photomultiplier at five wavelengths (306.3, 310.1, 313.5, 316.8 and 320.1 nm) using a blocking slit mask, which opens successively one of the five exit slits. The five exit slits are scanned twice within 1.6 s and this is repeated 20 times. The whole procedure is repeated five times for a total of about three minutes. The total ozone column is obtained from a combination of measurements at 310.1, 313.5, 316.8 and 320.1 nm weighted with a predefined set of constants



Discussion Paper | Discussion Paper | Discussion Paper | Discussion Paper |

AMTD

3, 2743–2778, 2010

chosen to minimize the influence of $SO_2$ and linearly varying absorption features such as from clouds or aerosols (Brewer manual, 1999; Gröbner and Meleti, 2004). RMIB has two Brewers on the roof of its building in Uccle (50°48′ N, 4°21′ E, 100 m a.s.l.). Brewer#016 is a single monochromator Mark II model that was installed in Uccle in 1983. In 1989, the instrument was equipped with an automated azimuth and zenith pointing system, resulting in a higher observation frequency (Cheymol et al., 2006). Brewer#178 is a double monochromator Mark III that was installed in September 2001. In addition to the standard observation routines, an additional routine was developed to be able to determine the AOD at 340 nm with the double monochromator Brewer. More precisely, the sun scan routine was adapted to make scans between 335 nm and 345 nm. The obtained spectral data are convoluted with the band pass function of the Cimel filter (standard Cimel filter values; Barr Associates Inc.). The data of this type, available since 17 August 2006, allow retrieving the AOD at 340 nm.

The Cimel sun photometer, which belongs to BISA (Belgium Institute of Space Aeronomy), is located at approximately 100 m from the Brewer instrument. It is an automatic sun-sky scanning filter radiometer allowing the measurements of the direct solar irradiance at wavelengths 340, 380, 440, 500, 670, 870, 940 and 1020 nm. These solar extinction measurements are used to compute Aerosol Optical Depth at each wavelength except for the 940 nm channel, which is used to retrieve total atmospheric column precipitable water in centimeters. The instrument is part of the AERONET network (http://aeronet.gsfc.nasa.gov/; Holben et al., 2001).

## 3 Method

To derive the AOD at 340 nm from the measurements described above, we apply the Langley Plot method in a similar way as described in Cheymol and De Backer (2003). The Langley Plot method is a linear regression technique that can be used for the retrieval of the Aerosol Optical Depth from direct radiation measurements. Only the basics of this method and the deviations from the algorithm in Cheymol and De Backer





AMTD
3, 2743–2778, 2010

(2003) will be described here. Details can be found in Cheymol and De Backer (2003) and in Marenco et al. (2002).

### 3.1 Basic equation

An important difference between this work and the one by Cheymol and De Backer (2003) is that the latter uses the direct sun measurements from the Brewer instrument for the received signal values, whereas here we use sun scans between 335 and 345 nm, convoluted with the band pass function of the Cimel filter at 340 nm. The use of the sun scans is an important improvement that simplifies the comparison of the AOD values, since it is no longer necessary to extrapolate the Cimel AOD values to the Brewer wavelength. Another advantage is that the intensities at this wavelength are larger due to the lower absorption by ozone, improving the signal to noise ratio. The signal, received by the Brewer instrument, is governed by Beer's law (using the notations as in Cheymol and De Backer, 2003):

$$S(\lambda) = K(\lambda) I_0(\lambda) \exp\left[-\mu\alpha(\lambda,T)\Omega - m\beta(\lambda)\frac{P}{P_{\mathrm{std}}} - \delta(\lambda)\sec(z_{\mathrm{a}})\right], \tag{1}$$

with $S(\lambda)$ the received signal, $K(\lambda)$ the proportionality factor of the instrument's response to the incoming solar radiation at wavelength $\lambda$, $I_0(\lambda)$ the irradiance outside the Earth's atmosphere at wavelenght $\lambda$, $\mu$ the relative optical airmass of the ozone layer at height=22 km, $\alpha(\lambda,T)$ the ozone absorption coefficient at wavelength $\lambda$ and temperature $T$, $\Omega$ the equivalent thickness of the ozone layer, $m$ the relative optical airmass of the atmosphere in a thin layer assumed to be at an altitude of 5 km for Rayleigh scattering, $\beta(\lambda)$ the Rayleigh scattering coefficient, $P_{\mathrm{std}}$ the standard pressure (1013.25 hPa), $P$ the station pressure (1000 hPa), $\delta(\lambda)$ the aerosol scattering optical thickness of a vertical path through the atmosphere and $z_{\mathrm{a}}$ the zenith angle of the sun.

This law reflects that, while passing through the atmosphere, the intensity of the direct beam at the top of the atmosphere is subject to absorption and scattering through three different physical phenomena: (a) absorption by ozone, (b) scattering by air





AMTD
3, 2743–2778, 2010

molecules (Rayleigh scattering) and (c) scattering by aerosol particles. The $SO_2$ absorption is not considered here, since this term is very low compared to the ozone absorption term, which is already small at 340 nm. To eliminate the dependence on the effective ozone temperature, the ozone absorption coefficient is computed using the effective ozone temperature (as in Cheymol and De Backer, 2003). This effective ozone temperature is calculated using ozone profiles from balloon soundings available at Uccle.

### 3.2 Langley plot method

Taking the logarithm of Eq. (1) gives Eq. (2):

$$\ln[S(\lambda)] + \mu\alpha(\lambda)\Omega + m\beta(\lambda)\frac{P}{P_{\mathrm{std}}} = \ln[K(\lambda)I_0(\lambda)] - \delta(\lambda)\sec(z_{\mathrm{a}})\,. \tag{2}$$

Let us define:

$$Y = \ln[S(\lambda)] + \mu\alpha(\lambda)\Omega + m\beta(\lambda)\frac{P}{P_{\mathrm{std}}}\,, \tag{3}$$

$$\mathrm{CF} = \ln[K(\lambda)I_0(\lambda)]\,, \tag{4}$$

$$A = -\delta(\lambda)\,, \tag{5}$$

$$X = \sec(z_{\mathrm{a}})\,. \tag{6}$$

(7)

With Eqs. (3)–(6), Eq. (2) can be simplified to

$$Y = \mathrm{CF} - A^{*}X\,. \tag{8}$$

Now, one AOD value ($-A$) and one calibration factor (CF) can be estimated per day. The quality of the linear regression depends on the range of the solar zenith angles covered during a certain day. Good observations at both high and low solar zenith angles are needed and the atmospheric conditions must remain stable over the day.

This leads to different criteria for the selection of the days on which the LPM can be applied (cloudless days). Cheymol et al. (2009) proposed the following criteria:

1. The individual DS data for which the air mass is above 3 are removed.

2. The ozone column and its standard deviation are computed on each group of 5 individual DS measurements for each wavelength. Data are accepted if the standard deviation is lower than 2.5 DU.

3. The range of zenith angles covered by valid DS observations for one day must be at least 20°.

4. The number of individual DS data must be at least 50 per day (i.e. 10 sequences of 5 observations).

Since in our case sun scans are used instead of DS measurements, these criteria have to be adapted. The test done on the ozone values (2nd criterion) loses its significance since the ozone observations of Brewer#178 and the sun scans between 335 nm and 345 nm are not performed simultaneously. Clouds are thus able to influence the intensity measurements during the sun scan, while the closest ozone observations (in time) could be made under cloudless conditions. The remaining criteria are applied to the sun scans instead of to DS measurements.

Manually verifying whether the selected days are indeed cloudless showed that these criteria were not sufficient. An additional criterion is therefore proposed. It is based on the ratio of the observed and expected intensities for a certain day. The observed intensities are obtained from the sun scans between 335 and 345 nm that are convoluted with the band pass function of the Cimel filter. The expected intensities (under cloudless circumstances) are calculated by the Tropospheric Ultraviolet and Visible Radiation Model (TUV model version 3.0; Madronich, 1993), which uses the band pass function of the Cimel filter at 340 nm. The climatological monthly mean total ozone value and a default constant AOD value are used as input parameters for the calculation of the monochromatic radiative transfer. The cloud optical depth and surface albedo are,





AMTD
3, 2743–2778, 2010

respectively 0 and 0.05. If a certain day is cloudless and the atmospheric conditions are stable, the ratio of the intensities should be more or less constant throughout the day (Fig. 1 shows the calculated ratios for a cloudless and for a cloudy day). In this context, a day is considered cloudless if the maximum deviation of the individual ratios (of a day) from the mean ratio is smaller than 20% (different threshold values were tested, but the 20% value generated the best results).

This leads to the following set of criteria for the selection of cloudless days (CCD=Criteria Cloudless Days) for the determination of the calibration factors with the Langley plot method:

1. The sun scans for which the air mass is above 3 are removed.

2. The range of zenith angles covered by the sun scans for one day must be at least 20°.

3. At least 10 sun scans per day have to remain after applying the first two criteria.

4. The maximum deviation of the individual ratios (of the observed and expected intensities) from the mean ratio for a certain day has to be smaller than 20%.

After applying these criteria, the selected cloudless days are used to determine the calibration coefficient of the instrument. With this calibration coefficient, the AOD can now be calculated for each individual observation. To avoid the influence of clouds on the calculated AOD values, we only calculated AOD values for the individual sun scans for which a direct sun observation, made with Brewer#178, is available within a time period of 5 min. It has to be mentioned that this however does not exclude all cloud-perturbed measurements. This is shown in the resulting AOD values, some of which seemed too high to be reliable. As the definition of simple criteria to detect cloud interference in the UV is complex (Dürr and Philipona, 2004) we propose at this stage only a manual method to exclude this cloud contamination. The application of a more sophisticated and automated method will be the subject of a subsequent study. Figure 2 shows the scatter plot of the Brewer AOD measurements and the corresponding Cimel





AMTD
3, 2743–2778, 2010

Brewer AOD measurements at 340 nm

V. De Bock et al.

measurements (with a maximum time difference of 30 min). There is a good agreement between Brewer and Cimel for Brewer AOD values lower than 2. When the AODs become larger than 2, there is virtually no agreement between the measurements of the two instruments. Based on this result, we decided to automatically remove all AOD values larger than 2 from our results on the assumption that they were influenced by clouds.

A set of criteria to select the individual clear sky AOD values (from all the calculated AOD values), can now be defined (CICA= Criteria Individual Clear sky AOD):

1. A direct sun observation must be available for each individual AOD measurement within a time period of 5 min.

2. Each individual AOD value must be lower than 2. Larger values are removed from the results.

The remaining AOD values were compared to quasi-simultaneous Cimel AODs at 340 nm (AERONET level 1.5 data). Only quasi-simultaneous measurements of both instruments (with a maximum time difference of 3 min) are considered. The AOD values from Brewer#178 at 320 nm were also compared to quasi-simultaneous Cimel values. Angström's law was applied to the Cimel measurements to extrapolate the values to 320 nm.

## 4 Results and discussion

### 4.1 Comparison between Brewer and Cimel measurements

For the comparison with the AOD values from the Cimel, the Brewer#178 sun scan measurements at 340 nm from September 2006 until May 2009 were used. For this period, a total of 12 cloudless days (Table 1) were selected using CCD (as mentioned in Sect. 3.2) combined with individual inspection. The mean calibration factor (CF) for these days is 18.579±0.084. With this calibration coefficient, the individual clear





AMTD
3, 2743–2778, 2010

sky AOD values (according to CICA) are calculated, using the Brewer#178 sun scans. The applied method resulted in 2059 AODs at 340 nm for a period from September 2006 to May 2009. Only quasi-simultaneous measurements from Brewer and Cimel (level 1.5 data from AERONET) were used for comparison. The remaining 274 quasi-simultaneous values Brewer and Cimel AODs at 340 nm had a correlation coefficient of 0.861 (Fig. 3). Selecting only those Brewer AOD observations with a concurrent Cimel observation (maximum time difference of 3 min) and with a quasi-simultaneous DS measurement (maximum time difference of 5 min) automatically eliminates most of the cloudy conditions. The scatter plot of the compared AODs still showed the presence of a few outliers (highlighted in red in Fig. 3), causing the rather low correlation coefficient compared to the one obtained by Cheymol et al. (2009) (correlation coefficient of 0.96 for the comparison between Brewer#016 at 320 nm and Cimel at 340 nm). These remarkable outliers solicit for further examination. We consider a single point in the scatter plot to be an outlier if the difference in AOD between Brewer and Cimel measurements is bigger than 0.5. All the sun scan measurements of days with an outlier were plotted. Figure 4 shows the theoretical and the observed relative intensity for a day on which an outlier was present (13 September 2006). The figure clearly shows that the outlier measurement (highlighted in red) is influenced by clouds. This justifies the removal of this point from the comparison. Similar checks were performed for the other outliers and it turned out that for those outliers, the Brewer measurements were made under cloud-perturbed circumstances. Then a comparison was made excluding these outliers. This resulted in a much higher correlation coefficient of 0.960. The slope is $0.992\pm0.018$ and the intercept is $0.005\pm0.008$ (Fig. 3), confirming a very good linear agreement between the AOD measurements of both instruments. The agreement between the AODs at 340 nm is better than at 320 nm (Fig. 5), where the correlation is 0.915, the slope $0.964\pm0.016$ and the intercept $0.006\pm0.007$. This shows that good quality AOD observations can be obtained at 340 nm from Brewer#178 with the proposed method.





AMTD
3, 2743–2778, 2010

## 4.2 AOD variability in Uccle on different timescales

A total of 2482 individual AOD measurements from Brewer#178 were calculated for the period between September 2006 and December 2009 and the values were examined for possible variations on seasonal, monthly and weekly timescales. Some of the individual AOD values were questionable, especially the values larger than 1.5. When Brewer and Cimel measurements were compared, these values were automatically removed from the results because the Brewer AOD values larger than 1.5 did not have a concurrent Cimel measurement. However, for the study of the individual values (which are not compared to the Cimel data) it is required to manually check the data for cloud-perturbed measurements. This manual cloud screening showed that most of the values larger than 1.5 were calculated under cloudy circumstances. These AOD values were removed from our results. So, next to the automatic cloud screening (using CICA), a manual check is done for the individual AOD values larger than 1.5. (An objective method to remove observations affected by clouds is under development.) The remaining 2393 individual AOD values were used to study variability on different time scales.

### 4.2.1 Seasonal and monthly variability

Many studies that investigate the seasonal variability of aerosols, report high AODs during summer (June, July, August) and spring (March, April, May) and low AODs in winter (December, January, February) and autumn (September, October, November). In Valencia (Spain), maximum AOD values were observed (between 2002–2005) from June to September, whereas the minimum values occurred from October to February (mainly in December and January) (Estellés, 2008). Behnert et al. (2004) observed two peak periods in the AOD values from Helgoland Island, Hamburg, Oostende and Lille. They occurred during spring (April–May) and summer (July–August). Studies in Ispra (Italy), Granada (Spain), M'Bour (Senegal), Gwangju (Korea) and Thessaloniki (Greece) also show high AOD values in summer and low values in winter (Meleti and





AMTD
3, 2743–2778, 2010

Cappellani, 2000; Léon et al., 2009; Lyamani et al., 2010; Kim et al., 2006; Kazadzis et al., 2007). (The latitude and longitude of the places mentioned in this article can be found in Table 2.)

The obtained AODs from Brewer#178 at Uccle are consistent with these studies. Figure 6 displays the mean seasonal AOD values for Uccle. The highest values can be observed in summer (respectively 0.64(±0.35), 0.59(±0.34) and 0.54(±0.27) for 2007, 2008 and 2009) and spring (respectively 0.56(±0.32), 0.61(±0.39) and 0.64(±0.38) for 2007, 2008 and 2009). This can also be derived from the histograms in Fig. 7. In winter more than 50% of the AODs at Uccle are below 0.3 and in summer more than 50% of the values are above 0.5. This is in agreement with the results from Kazadzis et al. (2007) for Thessaloniki, Greece. On a monthly scale (Fig. 8), the lowest AODs are observed in December (respectively 0.29(±0.22), 0.07(±0.02) and 0.23(±0.14) for 2007, 2008 and 2009), whereas the highest values occur in June (0.8(±0.38) in 2007) and April (0.74(±0.31) in 2008 and 0.78(±0.41) in 2009).

Possible explanations for the higher summer AODs are given by several authors. Behnert et al. (2004) attribute the summer peak values to the slowing down of air mass circulation in summer and the production of smog. This results in an accumulation of high aerosol concentrations above midlatitude regions. Kaskaoutis et al. (2007) explain the higher summer AODs at Ispra as a result of the absence of wet removal processes. According to Kazadzis et al. (2007), the enhanced evaporation and the higher temperatures during summer in Thessaloniki cause a rise in the turbidity of the boundary layer. Combined with stagnating weather systems, this will lead to the formation of aerosols. In winter, there is a significant amount of wet deposition of aerosols, which will cause a cleaning of the atmosphere and therefore lower AOD values. Koelemeijer et al. (2006) also state that high precipitation in winter leads to low AOD values. They observed an anti-correlation (−0.41 for the region of Belgium and The Netherlands) between precipitation and mean monthly AOD. We calculated a correlation of −0.24 between the mean monthly AOD and the monthly percentage of rain days at Uccle for a period between 1984 and 2009. The used AOD values are calculated from





AMTD
3, 2743–2778, 2010

Brewer#016 observations at 320 nm, since our time series from Brewer#178 at 340 nm is too short. In order to get a better view of the possible relationship between AOD and precipitation, we divided the calculated AOD values from 1984 to 2009 in two categories, “dry AODs” and “wet AODs”, based on the influence of precipitation on the values. We considered a single AOD value to be wet if precipitation was observed on this day or on the previous day. If both days were precipitation-free, we considered the AOD value to be representative for a dry day. Figure 9 shows the mean monthly AOD for the dry and for the wet days. It can be seen that during winter and early spring (November–April) the dry AODs are clearly higher than the wet values. The difference is less obvious for the summer and autumn months. This could be due to the rather frequent occurrence of local thunderstorms in these seasons, causing only local deposition of aerosols. Air flowing from other places can transport aerosol masses that were not influenced by these local thunderstorms and the measured AOD can thus be higher than one would expect based on the precipitation associated with the thunderstorms. In winter, precipitation is mainly related to the passage of large frontal systems. The wet deposition of the aerosols will thus be spread over a larger region. According to Cheymol and De Backer (2003), a relation with a pollution cycle or with a general circulation could be an explanation of the annual cycle in AOD at Uccle. The seasonal variation of the mixing height, which is smaller in winter and autumn, could be another explanation for the lower AOD in winter and autumn compared to summer and spring where the mixing layer height is thicker. The correlation between the monthly mean mixing height (Fig. 10) and the monthly mean AOD is 0.701 for Uccle. The correlation decreased strongly when the daily mean mixing height and the daily mean AOD are compared (correlation of 0.196).

#### 4.2.2 Weekly periodicity

Bäumer et al. (2008) and Xia et al. (2008) observed a weekly AOD cycle in Central Europe. They recorded the lowest values on Sunday and Monday, whereas higher values occurred between Wednesday and Saturday. This cycle is greater for the urban sites





AMTD
3, 2743–2778, 2010

than for the rural sites. For our measurements in Uccle, there is only a weak signal for such a weekly cycle (Table 3). The largest difference in mean AOD value occurs between Monday and Friday (respectively 0.48 versus 0.55). However, this difference is not statistically significant since the calculated t-value (1.32) is smaller than the theoretical t-value of 1.98 for the 95% confidence level (at 150 degrees of freedom). All the others t-values were smaller than this value and thus also not statistically significant. The t-value is calculated using Eq. (8) (Brandt, 1970).

$$t = \frac{\overline{x} - \overline{y}}{s_\Delta}, \tag{9}$$

where

$$s_\Delta^2 = \frac{N_x + N_y}{N_x N_y (N_x N_y - 2)} [(N_x - 1)s_x^2 + (N_y - 1)s_y^2] \tag{10}$$

$\overline{x}, s_x$ and $N_x$ the mean, standard deviation and number of $x_i$
$\overline{y}, s_y$ and $N_y$ the mean, standard deviation and number of $y_i$

It has to be mentioned that the AOD values are not perfectly normal distributed (which is a condition for applying the t-test), but they are close to a normal distribution. The skewness and kurtosis are, respectively 1.13 and 1.33 and 5.1% of all the values is situated in the interval $[\mu - 2\sigma; \mu + 2\sigma]$.

## 5 Summary and conclusions

Aerosols are the most important source of uncertainty in current climate change research (IPCC, 2007). Therefore knowledge of optical and physical properties of aerosols, such as the Aerosol Optical Depth, is essential to gain a better understanding in their effects. In this perspective, a new method was developed to retrieve AOD values at 340 nm from Brewer#178 sun scan measurements at Uccle, which allowed for a direct comparison with AOD values from the co-located Cimel sun photometer at the





AMTD
3, 2743–2778, 2010

same wavelength. The AOD retrieval method was based on the Langley Plot Method (as described in Cheymol and De Backer, 2003). For this linear regression technique, the cloudless days in the time period for which the AOD is to be calculated, have to be selected. The criteria from Cheymol et al. (2009) had to be adapted so that they could be applied on sun scan measurements instead of direct sun measurements. Also, a new criterion, based on the ratio of the observed and expected intensities for a certain day, was added since the adapted criteria were not sufficient. This led to a new set of criteria for the selection of the cloudless days (CCD). The selected cloudless days were then used to determine the calibration coefficient of the instrument. With this coefficient, the individual clear sky AOD values (selected using CICA) were calculated from the Brewer sun scans. These values were then compared to the AOD values from the Cimel. After removing the outliers from the comparison, the correlation between the Brewer#178 and Cimel measurements was 0.96, the slope was 0.992±0.018 and the intercept was 0.005±0.008. This proves that there is a very good linear agreement between the AOD measured by both instruments and that good quality AOD observations can be obtained at 340 nm from the sun scans of Brewer#178. The seasonal and monthly variability of the Brewer AODs is consistent with other studies that report on higher AOD values during spring and summer and lower values in autumn and winter. No clear weekly cycle is present for the measurements in Uccle.

Still some AOD measurements may exist that are perturbed by clouds, which are not removed by the automatic and manual cloud screening. Currently, the automatic cloud screening selects the sun scan measurements that have a direct sun measurement within a time period of 5 min for the calculation of the AOD. The individual AOD measurements larger than 2 are automatically removed from the results, since these values are very unlikely for our location. During the manual screening, AOD values larger than 1.5 are removed when the scatter plot of the relative intensities (i.e. photon counts) shows that the AODs are calculated under cloudy circumstances. The influence of scattered clouds on our measurements is still an issue for the calculation of the AOD values and the current cloud-screening algorithm has to be improved to further





AMTD
3, 2743–2778, 2010

increase the quality and reliability of the data.

*Acknowledgements.* This research was performed under the project AGACC contract SP/AT/01B of the Belgian Science Policy. We thank Christian Hermans (Belgian Institute for Space Aeronomy, Belgium) for establishing and maintaining the AERONET site at Uccle. Our thanks also go to Roeland Van Malderen (Royal Meteorological Institute of Belgium, Belgium) for his constructive advice concerning data analysis and interpretation.

## References

Andreae, M. O., Jones, C. D., and Fox, P. M.: Strong present-day aerosol cooling implies a hot future, Nature, 435, 1187–1190, doi:10.1038/nature03671, 2005. 2745

Arola, A. and Koskela, T.: On the sources of bias in aerosol optical depth retrieval in the UV range, J. Geophys. Res., 109, D08209, doi:10.1029/2003JD004375, 2004. 2746

Bais, A. F.: Absolute spectral measurements of direct solar ultraviolet irradiance with a brewer spectrophotometer, Appl. Optics, 36(21), 5199–5204, doi:10.1364/AO.36.005199, 1997. 2746

Bäumer, D., Rinke, R., and Vogel, B.: Weekly periodicities of Aerosol Optical Thickness over Central Europe – evidence of an anthropogenic direct aerosol effect, Atmos. Chem. Phys., 8, 83–90, doi:10.5194/acp-8-83-2008, 2008. 2746, 2757

Behnert, I., Matthias, V., and Doerffer, R.: Aerosol optical thickness and its spectral dependence derived from sun photometer measurements over the southern North Sea coastal region, Óptica pura y aplicada, 37(3), 3253–3257, 2004. 2746, 2755, 2756

Brandt, S.: Statistical and Computational Methods in Data Analysis, North-Holland Publishing Company, Amsterdam, The Netherlands, 1970. 2758

Brewer, A. W.: A replacement for the Dobson spectrophotometer, Pure Appl. Geophys., 106–108, 919–927, doi:10.1007/BF00881042, 1973. 2747

Brewer MKIII Spectrophotometer (double spectrometer): Operator's Manual. OM-BA-C231 REV B, 17 August, Kipp & Zonen Inc., Delft, The Netherlands, 1999. 2748

Cazorla, A., Shields, J. E., Karr, M. E., Olmo, F. J., Burden, A., and Alados-Arboledas, L.: Technical Note: Determination of aerosol optical properties by a calibrated sky imager, Atmos. Chem. Phys., 9, 6417–6427, doi:10.5194/acp-9-6417-2009, 2009. 2746





AMTD

3, 2743–2778, 2010

Che, H., Zhang, X., Chen, H., Damiri, B., Goloub, P., Li, Z., Zhang, X., Wei, Y., Zhou, H., Dong, F., Li, D., and Zhou, T.: Instrument calibration and aerosol optical depth validation of the chinese aerosol remote sensing network, J. Geophys. Res., 114, D03206, doi:10.1029/2009JD011030, 2009. 2746

Cheymol, A. and De Backer, H.: Retrieval of the aerosol optical depth in the UV-B at Uccle from Brewer ozone measurements over a long time period 1984–2002, J. Geophys. Res., 108, D24, doi:10.1029/2003KD003758, 2003. 2744, 2746, 2747, 2748, 2749, 2750, 2757, 2759

Cheymol, A., De Backer, H., Josefsson, W., and Stübi, R.: Comparison and validation of the aerosol optical depth obtained with the Langley plot method in the UV-B from Brewer ozone spectrophotometer measurements, J. Geophys. Res., 111, D16202, doi:10.1029/2006JD007131, 2006. 2748

Cheymol, A., Gonzalez Sotelino, L., Lam, K. S., Kim, J., Fioletov, V., Siani, A. M., and De Backer, H.: Intercomparison of Aerosol Optical Depth from Brewer Ozone spectrophotometers and CIMEL sunphotometers measurements, Atmos. Chem. Phys., 9, 733–741, doi:10.5194/acp-9-733-2009, 2009. 2746, 2751, 2754, 2759

Cordero, R. R., Seckmeyer, G., Pissulla, D., and Labbe, F.: Exploitation of spectral direct UV irradiance measurements, Metrologia, 46, 19–25, doi:10.1088/0026-1394/46/1/003, 2009. 2745

Corr, C. A., Krotkov, N., Madronich, S., Slusser, J. R., Holben, B., Gao, W., Flynn, J., Lefer, B., and Kreidenweis, S. M.: Retrieval of aerosol single scattering albedo at ultraviolet wavelengths at the T1 site during MILAGRO, Atmos. Chem. Phys., 9, 5813–5827, doi:10.5194/acp-9-5813-2009, 2009. 2746

De Backer, H.: Time series of daily erythemal UV doses at Uccle, Belgium, Int. J. Remote Sens., 30(15), 4145–4145, doi:10.1080/01431160902852032, 2009. 2747

Diffey, B. L.: Solar ultraviolet radiation effects on biological systems, Phys. Med. Biol., 36(3), 299–328, doi:10.1088/00.31-9155-36-3-001, 1991. 2745

Dürr, B. and Philipona, R.: Automatic cloud amount detection by surface longwave downward radiation measurements, J. Geophys. Res., 109, D05201, doi:10.1029/2003JD004182, 2004. 2752

Estellés, V., Martinez-Lozano, J. A., Utrillas, M. P., and Campanelli, M.: Columnar aerosol properties in Valencia (Spain) by ground-based Sun photometry, J. Geophys. Res., 112, D11201, doi:10.1029/2006JD008167, 2008. 2746, 2755

Gröbner, J. and Meleti, C.: Aerosol optical depth in the UVB and visible wavelength range from

Brewer spectrophotometer direct irradiance measurements: 1991–2002, J. Geophys. Res., 109, D09202, doi:10.1029/2003JD004409, 2004. 2746, 2748

Hatzianastassiou, N., Ghikas, A., Mihalopoulos, N., Torres, O., and Katsoulis, B. D.: Natural versus anthropogenic aerosols in the Eastern Mediterranean Basin derived from multiyear TOMS and MODIS satellite data, J. Geophys. Res., 114, D24202, doi:10.1029/2009JD011982, 2009. 2747

Holben, B. N., Tanré, D., Smirnov, A., Eck, T. F., Slutsker, I., Abuhassan, N., Newcomb, W. W., Schafer, J. S., Chatenet, B., Lavenu, F., Kaufman, Y. J., Vande Castle, J., Setzer, A., Markham, B., Clark, D., Frouin, R., Halthore, R., Karneli, A., O'Neill, N. T., Pietras, C., Pinker, R. T., Voss, K., and Zibordi, G.: An emerging ground-based aerosol climatology: aerosol optical depth from AERONET, J. Geophys. Res., 106, D11, 12067–12097, doi:10.1029/2001JD900014, 2001. 2748

Intergovernmental Panel on Climate Change 2007: The physical science, Technical summary of the working group I report, Cambridge University Press, New York, 2007. 2745, 2758

Kaskaoutis, D. G., Kambezidis, H. D., Hatzianastassiou, N., Kosmopoulos, P. G., and Badarinath, K. V. S.: Aerosol climatology: on the discrimination of aerosol types over four AERONET sites, Atmos. Chem. Phys. Discuss., 7, 6357–6411, doi:10.5194/acpd-7-6357-2007, 2007. 2756

Kaufman, Y. J., Tanré, D., and Boucher, O.: A satellite view of aerosols in the climate system, Nature, 419, 215–223, doi:10.1038/nature01091, 2002. 2745

Kazadzis, S., Bais, A., Amiridis, V., Balis, D., Meleti, C., Kouremeti, N., Zerefos, C. S., Rapsomanikis, S., Petrakakis, M., Kelesis, A., Tzoumaka, P., and Kelektsoglou, K.: Nine years of UV aerosol optical depth measurements at Thessaloniki, Greece, Atmos. Chem. Phys., 7, 2091–2101, doi:10.5194/acp-7-2091-2007, 2007. 2746, 2756

Kazadzis, S., Bias, A., Kouremeti, N., Geraspoulos, E., Garane, K., Blumthaler, M., Schallhart, B., and Cede, A.: Direct spectral measurements with a Brewer spectroradiometer: absolute calibration and aerosol optical depth retrieval, Appl. Optics, 44(9), 1681–1690, doi:10.1364/AO.44.001681, 2005. 2746

Kerr, J. B., Asbridge, I. A., and Evans, W. F. J.: Intercomparison of total ozone measured by the Brewer and Dobson spectrophotometer at Toronto, J. Geophys. Res., 93, D9, 11129–11140, doi:10.1029/JD093iD09p11129, 1988. 2747

Kim, J. E., Kim, Y. J., and He, Z.: Temporal variation and measurement uncertainty of UV aerosol optical depth measured from April 2002 to July 2004 at Gwangju, Korea, Atmos.

Res., 81, 111–123, doi:10.1016/j.amosres.2005.11.006, 2006. 2746, 2756

Kim, J. E., Ryu, S. Y., and Kim, Y. J.: Determination of radiation amplification factor of atmospheric aerosol from the surface UV irradiance measurement at Gwangju, Korea, Theor. Appl. Climatol., 91, 217–228, doi:10.1007/s00704-006-0285-x, 2008. 2746

Kirchhoff, V. W. J. H., Silva, A. A., Costa, C. A., Paes Leme, N., Pavão, H. G., and Zaratti, F.: UV-B optical thickness observations of the atmosphere, J. Geophys. Res., 106, D3, 2963–2973, doi:10.1029/2000JD900506, 2001. 2746

Koelemeijer, R. B. A., Homan, C. D., and Matthijsen, J.: Comparison of spatial and temporal variations of aerosol optical thickness and particulate matter over Europe, Atmos. Env., 40, 5304–5315, doi:10.1016/j.atmosenv.2006.04.044, 2006. 2756

Léon, J.-F., Derimian, Y., Chiapello, I., Tanré, D., Podvin, T., Chatenet, B., Diallo, A., and Deroo, C.: Aerosol vertical distribution and optical properties over M'Bour (16.96° W; 14.39° N), Senegal from 2006 to 2008, Atmos. Chem. Phys., 9, 9249–9261, doi:10.5194/acp-9-9249-2009, 2009. 2746, 2756

Liu, S. C., McKeen S. A., and Madronich, S.: Effect of anthropogenic aerosols on biologically active ultraviolet radiation, Geophys. Res. Lett., 18(12), 2265–2268, doi:10.1029/91GL02773, 1991. 2745

Lohmann, U.: Possible aerosol effects on ice clouds via contact nucleation, J. Atmos. Sci., 59(3), 647–656, 2002. 2745

Lohmann, U. and Feichter, J.: Global indirect aerosol effects: a review, Atmos. Chem. Phys., 5, 715–737, doi:10.5194/acp-5-715-2005, 2005. 2745

Lyamani, H., Olmo, F. J., and Alados-Arboledas, L.: Physical and optical properties of aerosols over an urban location in Spain: seasonal and diurnal variability, Atmos. Chem. Phys., 10, 239–254, doi:10.5194/acp-10-239-2010, 2010. 2744, 2746, 2756

Madronich, S.: UV radiation in the natural and perturbed atmosphere, in: Environmental Effects of Ultraviolet Radiation, edited by: Teveni, M., Lewis, Boca Raton, FL., 17–69, 1993. 2751

Marenco, F., di Sarra, A., and Di Luisi, J.: Methodology for determining aerosol optical depth from Brewer 300–320 nm ozone measurements, Appl. Optics, 41(9), 1805–1814, doi:10.1364/AO.41.001805, 2002. 2746, 2749

Marenco, F., Santacesaria, V., Bais, A. F., Balis, D., di Sarra, A., Papayannis, A., and Zerefos, C.: Optical properties of tropospheric aerosols determined by lidar and spectrophotometric measurements (photochemical activity and solar ultraviolet radiation campaign), Appl. Optics, 36(27), 6875–6886, doi:10.1364/AO.36.006875, 1997. 2746

Meleti, C. and Cappellani, F.: Measurements of aerosol optical depth at Ispra: analysis of the correlation with UV-B, UV-A and total solar irradiance, J. Geophys. Res., 105(D4), 4971–4978, doi:10.1029/1999JD900459, 2000. 2746, 2755

Mulcahy, J. P., O'Dowd, C. D., and Jennings, S. G.: Aerosol optical depth in clean marine and continental northeast Atlantic air, J. Geophys. Res., 114, D20204, doi:10.1029/2009JD011992, 2009. 2746

Myrhe, G.: Consistency between satellite derived and modelled estimates of the direct aerosol effect, Science, 325(187), 187–190, doi:10.1126/science.1174461, 2009. 2745

Raghavendra Kumar, K., Narasimhulu, K., Balakrishnaiah, G., Suresh Kumar Reddy, B., Rama Gopal, K., Reddy, R. R., Satheesh, S. K., Krishna Moorthy, K., and Suresh Babu, S.: A study on the variations of optical and physical properties of aerosols over a tropical semi-arid station during grassland fire, Atmos. Res., 95, 77–87, doi:10.1016/j.atmosres.2009.08.012, 2010. 2744

Ramanathan, V., Crutzen, P. J., Kiehl, J. T., and Rosenfeld, D.: Aerosols, climate and the hydrological cycle, Science, 294, 2119–2121, doi:10.1126/science.1064034, 2001. 2745

Remer, L., Kleidmann, R. G., Levy, R. C., Kaufman, Y. J., Tanré, D., Mattoo, S., Vanderlei Martins, J., Ichoku, C., Koren, I., Yu, H., and Holben, B. N.: Global aerosol climatology from the MODIS satellite sensors, J. Geophys. Res., 113, D14S07, doi:10.1029/2007JD009661, 2008. 2746

Rieder, H. E., Holawe, F., Simic, S., Blumthaler, M., Krzyścin, J. W., Wagner, J. E., Schmalwieser, A. W., and Weihs, P.: Reconstruction of erythemal UV-doses for two stations in Austria: a comparison between alpine and urban regions, Atmos. Chem. Phys., 8, 6309–6323, doi:10.5194/acp-8-6309-2008, 2008. 2745

Sellito, P., di Sarra, A., and Siani, A. M.: An improved algorithm for the determination of aerosol optical depth in the ultraviolet spectral range from Brewer spectrophotometer observations, J. Opt. A-Pure Appl. Op., 8, 849–855, doi:10.1088/1464-4258/8/10/005, 2006. 2746

Tang, X., Madronich, S., Wallington, T., and Calamari, D.: Changes in tropospheric composition and air quality, J. Photoch. Photobio. B, 46, 83–95, doi:10.1039/b211086e, 1998. 2745

Taylor, T. E., L'Ecuyer, T. S., Slusser, J. R., Stephens, G. L., and Goering, C. D.: An operational retrieval algorithm for determining aerosol optical properties in the ultraviolet, J. Geophys. Res., 113, D03201, doi:10.1029/2007JD008661, 2008. 2746

Tevini, M. and Teramura, H. A.: UV-B effects on terrestrial plants, Photochem. Photobiol., 50, 479–487, doi:10.1111/j.1751-1097.1989.tb05552.x, 1989 2745





AMTD
3, 2743–2778, 2010

UNEP: Environmental effects of ozone depletion and its interactions with climate change: 2006 assessment, United Nations Evironment Programme, Nairobi, Kenya, 2006. 2745
Unger, N., Menon, S., Koch, D. M., and Shindell, D. T.: Impacts of aerosol-cloud interactions on past and future changes in tropospheric composition, Atmos. Chem. Phys., 9, 4115–4129, doi:10.5194/acp-9-4115-2009, 2009. 2744, 2745
Xia, X., Eck, T. F., Holben, B. N., Philippe, G., and Chen, H.: Analysis of the weekly cycle of aerosol optical depth using AERONET and MODIS data, J. Geophys. Res., 113, D14217, doi:10.1029/2007JD009604, 2008. 2746, 2757





AMTD
3, 2743–2778, 2010

Brewer AOD measurements at 340 nm

V. De Bock et al.

Title Page
Abstract | Introduction
Conclusions | References
Tables | Figures
◀| |▶
◀ ▶
Back | Close
Full Screen / Esc
Printer-friendly Version
Interactive Discussion

**Table 1.** List of selected cloudless days from September 2006 until May 2009.

| | | | |
|---|---|---|---|
| 6 Sep 2006 | 30 Apr 2007 | 5 Aug 2007 | 11 May 2008 |
| 4 Apr 2007 | 1 May 2007 | 5 May 2008 | 1 Jul 2008 |
| 22 Apr 2007 | 2 May 2007 | 8 May 2008 | 29 May 2009 |





AMTD
3, 2743–2778, 2010

Brewer AOD measurements at 340 nm

V. De Bock et al.

**Table 2.** List of places mentioned in this article with their latitude and longitude.

| Location | Latitude | Longitude |
|---|---|---|
| Uccle (Belgium) | 50°48′ N | 4°21′ E |
| Oostende (Belgium) | 51°13′ N | 2°55′ E |
| Lille (Belgium) | 50°36′ N | 3°06′ E |
| Helgoland Island (Germany) | 54°10′ N | 7°53′ E |
| Hamburg (Germany) | 53°34′ N | 9°56′ E |
| Ispra (Italy) | 45°49′ N | 8°38′ E |
| Valencia (Spain) | 39°30′ N | 0°25′ W |
| Granada (Spain) | 37°10′ N | 35°35′ E |
| Thessaloniki (Greece) | 40°30′ N | 22°54′ E |
| Beijing (China) | 39°59′ N | 116°19′ E |
| Gwangju (Korea) | 35°13′ N | 126°50′ E |
| M'Bour (Senegal) | 16°58′ N | 14°23′ E |





AMTD
3, 2743–2778, 2010

**Table 3.** Mean AOD values and their standard deviations for each day of the week.

| Day of the week | Mean AOD |
|---|---|
| Monday | 0.48±0.31 |
| Tuesday | 0.54±0.36 |
| Wednesday | 0.53±0.32 |
| Thursday | 0.54±0.40 |
| Friday | 0.55±0.33 |
| Saturday | 0.51±0.34 |
| Sunday | 0.51±0.35 |





AMTD
3, 2743–2778, 2010

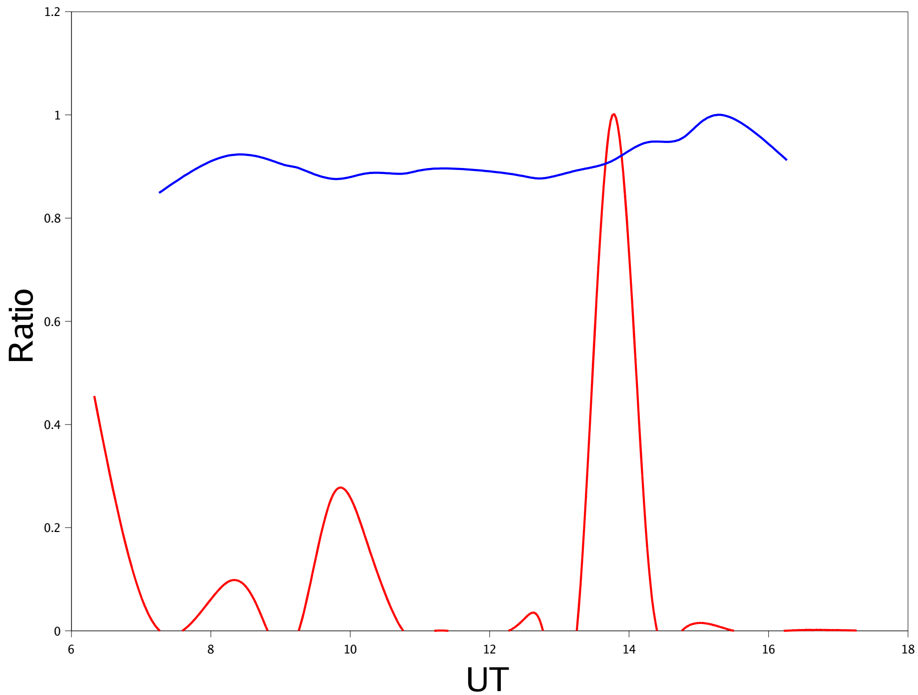


**Fig. 1.** Ratio of the observed and expected intensities for a cloudless (5 August 2007; in blue) and for a cloudy (20 July 2008; in red) day at Uccle.





AMTD
3, 2743–2778, 2010

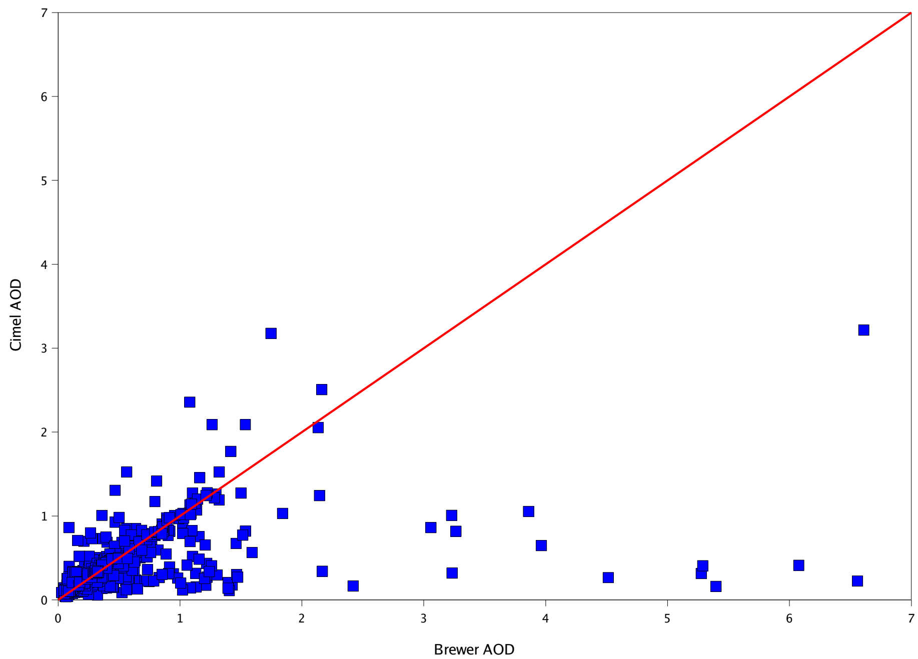


**Fig. 2.** Scatter plot of the Brewer and Cimel AOD at 340 nm (time period for the comparison is 30 min). The red curve represents $f(x)=x$.





AMTD
3, 2743–2778, 2010

Brewer AOD measurements at 340 nm

V. De Bock et al.

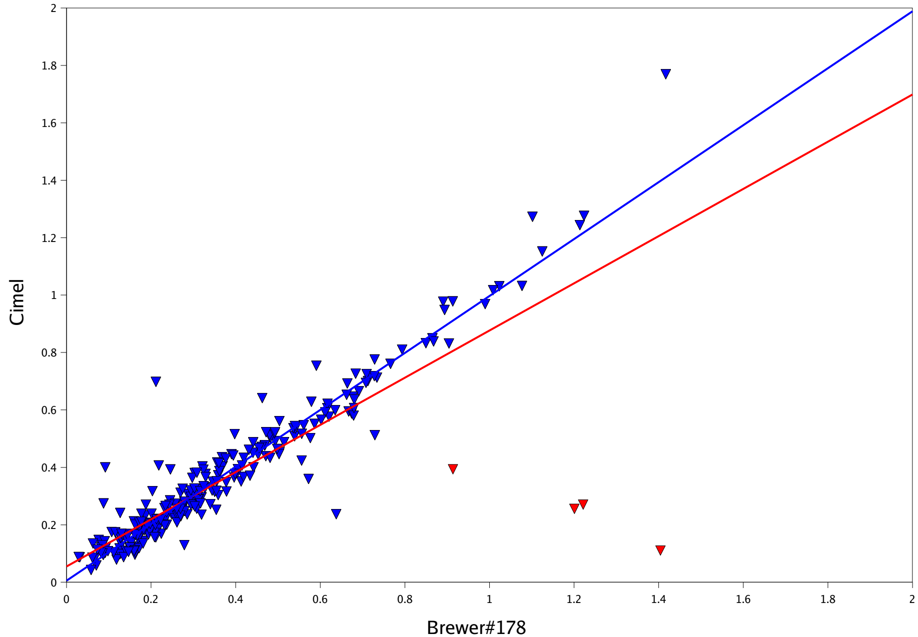


**Fig. 3.** Comparison of the Brewer and Cimel AOD values at 340 nm (time period for the comparison is 3 min). The red curve ($f(x)=0.822x+0.055$) represents all the data. The blue curve ($f(x)=0.992x+0.005$) shows the data without the outliers.





AMTD
3, 2743–2778, 2010

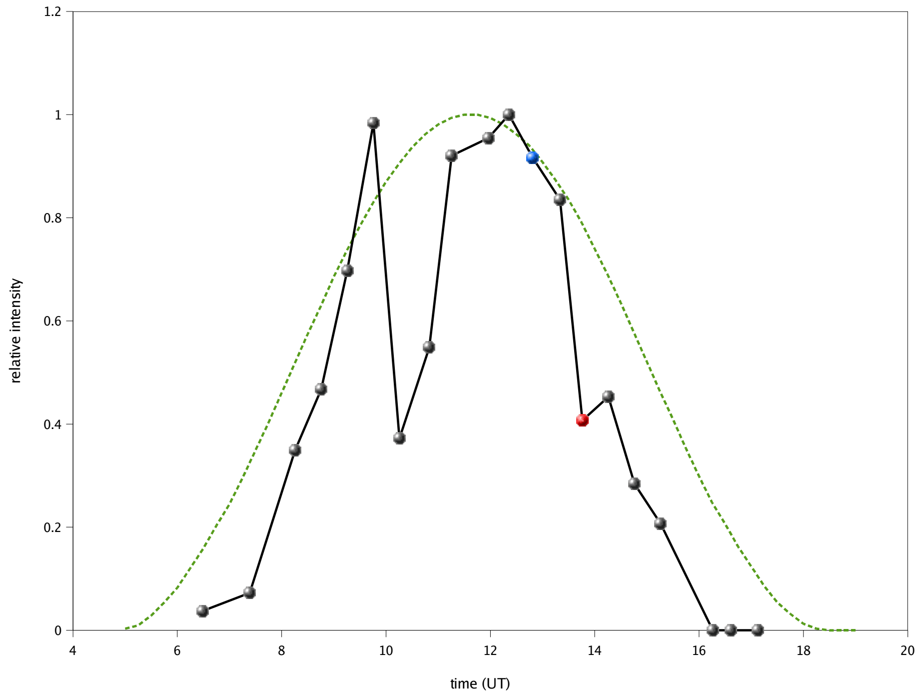


**Fig. 4.** Sun scan measurements of Brewer#178 on a day for which an outlier was present (13 September 2006). The green dashed line represents the theoretical values, based on the output of the TUV model, whereas the black line represents the observed relative intensities. The highlighted points (red and blue) represent the points for which the comparison with the Cimel measurements was done (which means there was a Cimel observation within a time period of 3 min). The difference between the Brewer and Cimel measurements was larger than 0.5 for the red point, which was considered to be an outlier. From this plot, it is clear that this outlier measurement is strongly influenced by clouds.





AMTD
3, 2743–2778, 2010

Brewer AOD measurements at 340 nm

V. De Bock et al.

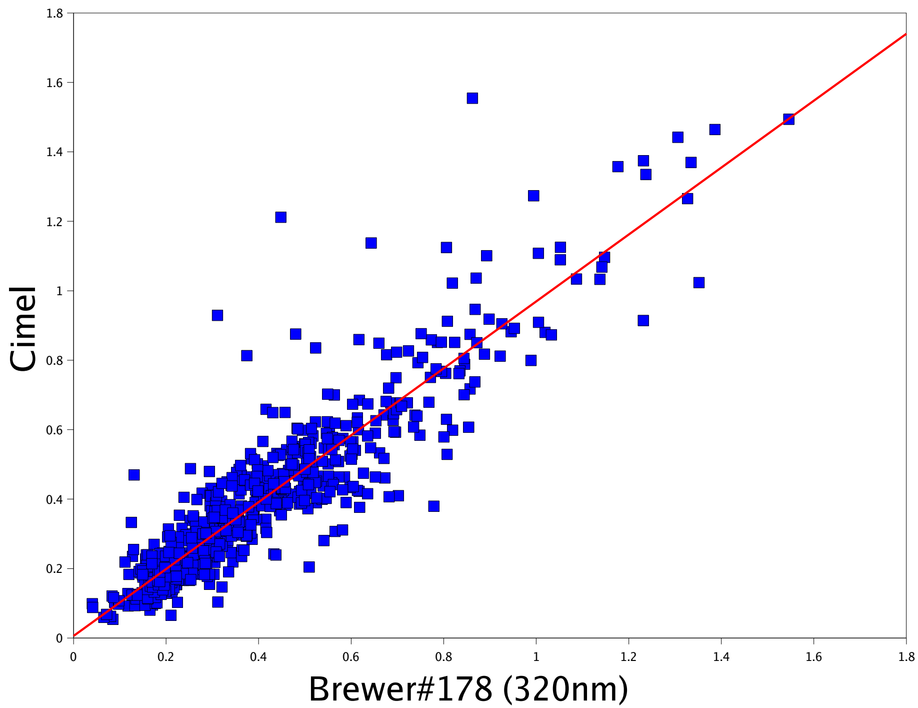


**Fig. 5.** Comparison of the Brewer#178 and Cimel values at 320 nm. The red line is the linear regression curve ($f(x)=0.964x+0.006$) of the comparison.

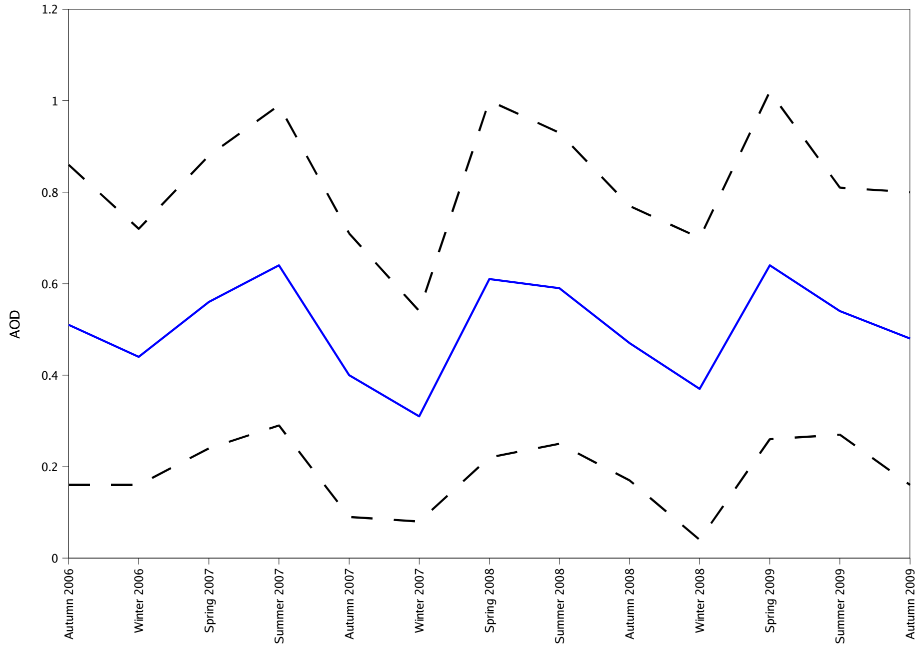


**Fig. 6.** Seasonal variation in AOD at Uccle (based on data from September 2006 to December 2009). The blue line is the mean seasonal value, whereas the dashed black lines represent the mean value ± its standard deviation.





AMTD
3, 2743–2778, 2010

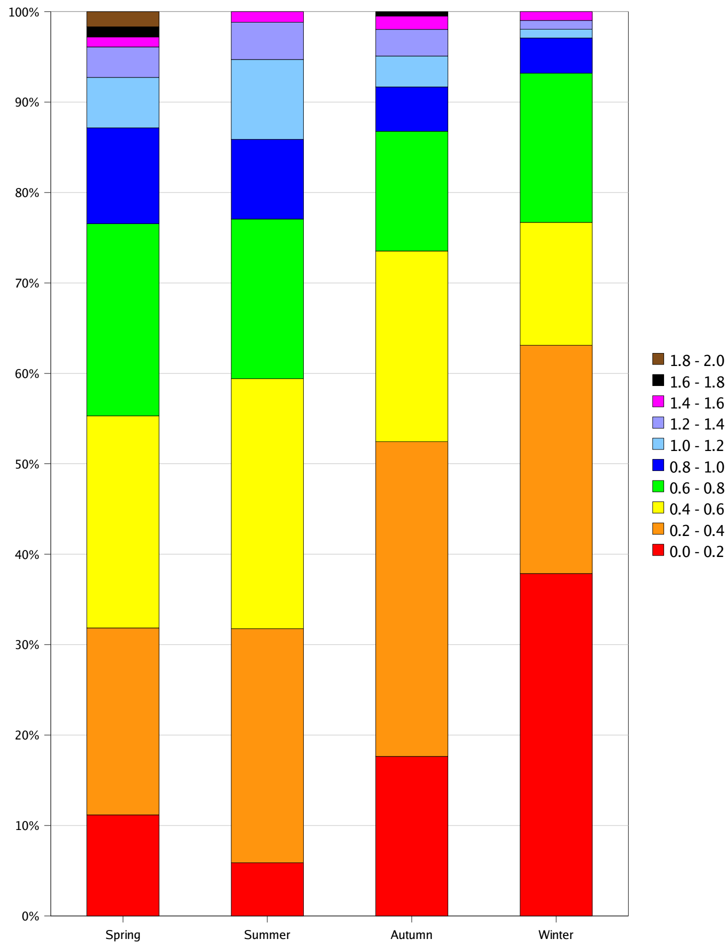


**Fig. 7.** Seasonal frequency distribution of AOD values at 340 nm at Uccle between 2006 and 2009.





AMTD
3, 2743–2778, 2010

Brewer AOD measurements at 340 nm

V. De Bock et al.

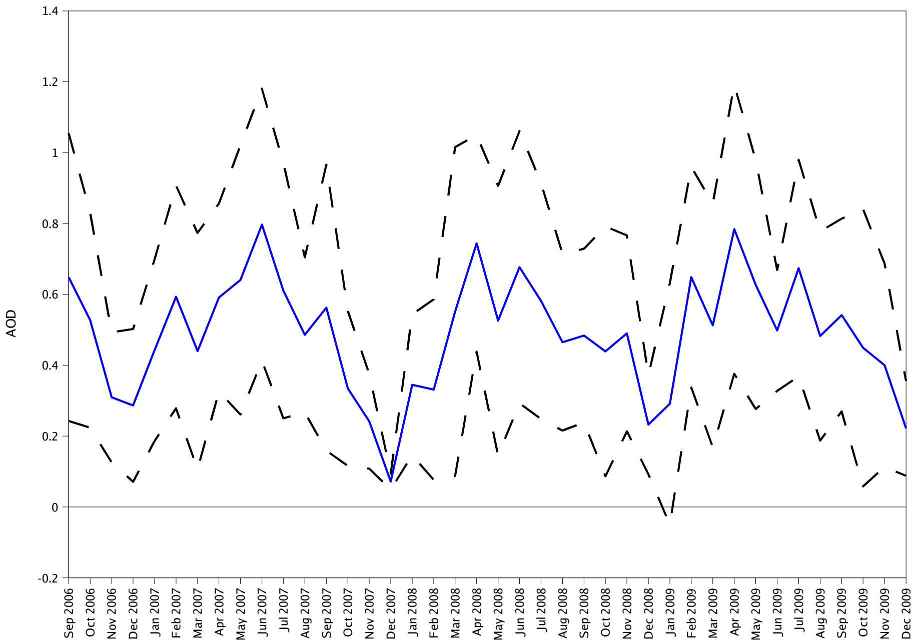


**Fig. 8.** Monthly variation in AOD at Uccle (based on data from September 2006 to December 2009). The blue line is the mean seasonal value, whereas the dashed black lines represent the mean value ± its standard deviation. For December 2007, the mean monthly value is based on only 3 individual AOD values. This explains the low standard deviation for this month.





AMTD
3, 2743–2778, 2010

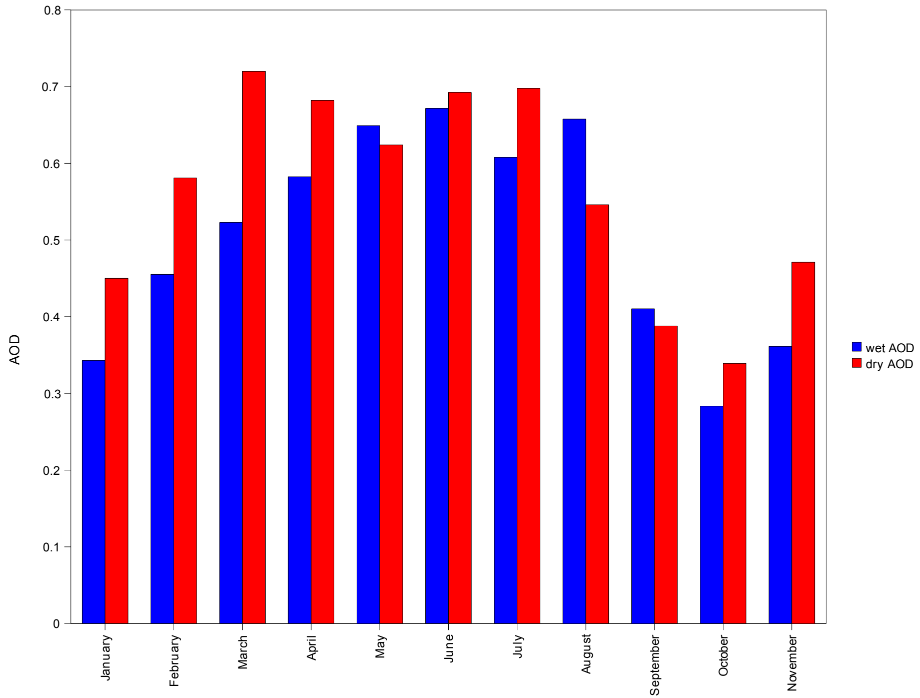


**Fig. 9.** Mean monthly AOD values (at 320 nm from Brewer#016) for dry and wet days for a time period from 1984 to 2009.





AMTD
3, 2743–2778, 2010

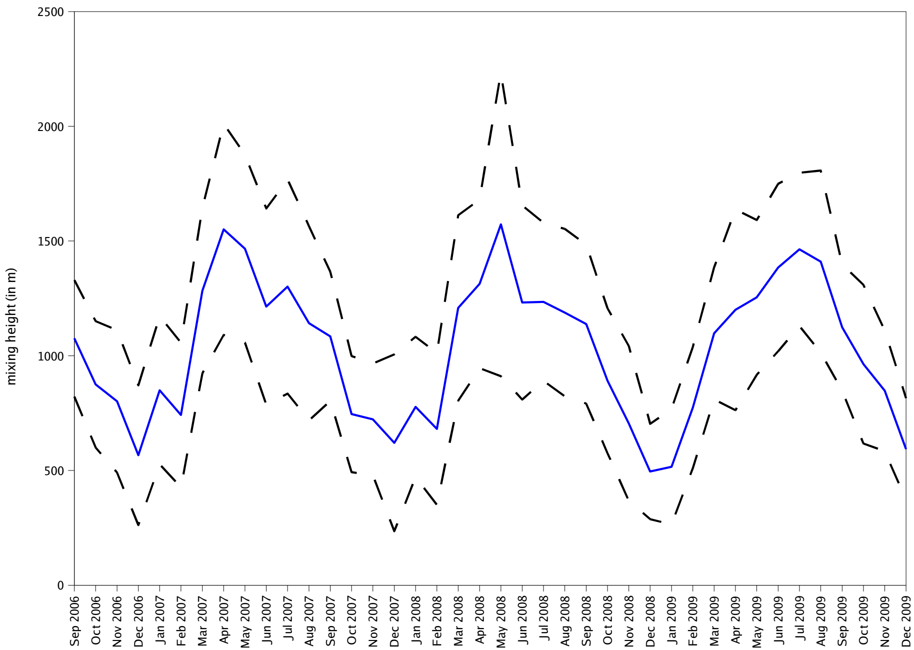


**Fig. 10.** Monthly mean mixing height for Uccle (ECMWF). The blue line is the mean seasonal value, whereas the dashed black lines represent the mean value ± its standard deviation.